

# GEOMETRY AND DIFFRACTION EFFECTS IN ACOUSTIC BEAM REFLECTION STUDIES FROM A FLUID-LOADED PLATE

O.I. Lobkis, A. Safaeinili<sup>1</sup> and D.E. Chimenti<sup>†</sup>  
Center for NDE and  
<sup>†</sup>Aerospace Engrg & Engrg Mechanics Dept  
Iowa State University  
Ames IA 50011

## INTRODUCTION

The near coincidence of the guided wave modes of a plate with zeroes of the reflection coefficient has been used often in the past [1-4] to estimate the plate's guided wave mode spectrum. Schoch [5] in his quantitative treatment of acoustic reflection from plates expresses the reflected field as a one-dimensional spectral integral over the incident field weighted by the reflection coefficient (RC) and by a propagator term which accounts for diffraction in the incident plane. Bertoni and Tamir [6] later evaluated this integral approximately for an incident Gaussian beam in their analysis of leaky Rayleigh waves. This procedure was later extended to reflection from plates, by Pitts, *et al.* [7]. Comparisons between numerical or analytical evaluations of this integral formulation of the reflected field and experimental measurements have been made by several authors. A missing element in essentially all these prior treatments, however, is a rigorous analysis of the influence of the receiving transducer.

A three-dimensional calculation of beam reflection from fluid-loaded plates is presented here, in which the spectral integrals are evaluated by uniform asymptotic analysis, to properly account for beam incidence close to a plate mode [8]. This procedure, which is specialized from a recent approximate treatment of beam reflection from planar and curved interfaces, permits the inclusion of transducer diffraction effects of both the transmitter and receiver in a completely general fashion, while providing a straightforward analytical expression for the voltage at the receiver. We find that the coincidence of the RC zeroes with the observed reflection minima can depend on the transducer width and experimental geometry, in some cases

---

<sup>1</sup>Present address: Rockwell International Science Center, Thousand Oaks, CA 91360

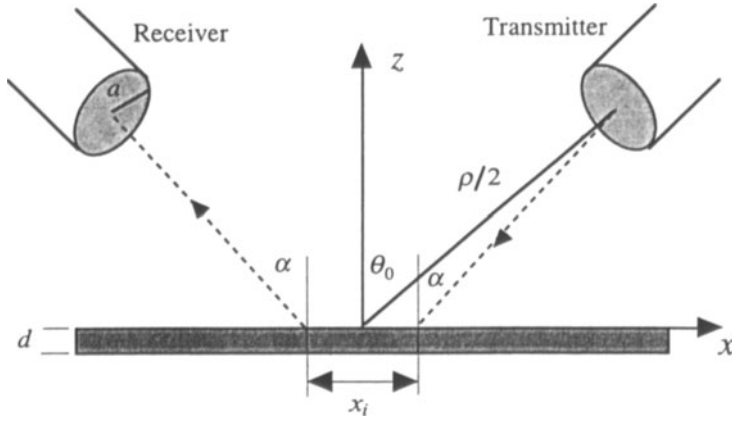


Figure 1: Schematic of experimental geometry for analysis of beam reflection from fluid-loaded structures; incident angle is  $\alpha$ ,  $\rho$  is the total water path, and  $x_i$  is the beam shift parameter. The plate is infinite in the  $y$  direction.

strongly so. As a demonstration we also report here a series of precision experiments on a uniform, homogeneous plate to validate our calculation and expose any possible limitations. In general, we have obtained excellent detailed agreement with theory in many experiments, which could be exploited to infer material properties through inversion of experimental data [9].

## THEORY

The geometry for the analysis presented here is shown in Fig.1. The system consists of two identical planar transducers of radius  $a$  (transmitter and receiver) immersed in liquid and oriented at equal and opposite angles  $\alpha$  from the normal. A solid isotropic plate of thickness  $d$  is located a distance  $z_0$  from the center of the transducer faces. The distance between points of intersection of the transducer acoustical axes on the upper plate surface is denoted by  $x_i$ . The origin of coordinates bisects  $x_i$  and lies on the upper plate surface, as seen in the figure.

The incident  $i$  or reflected  $r$  transducer fields  $\Psi_{i,r}$  at an arbitrary point  $(x, y, z)$  can be expressed through the Rayleigh integral formula for the field of a planar transducer using the transducer directivity function  $F_T(\theta, \phi)$ , which depends on transducer position and orientation. According to the Auld reciprocity formula [10], the output signal of the receiving transducer can be represented as an integral over the receiver surface  $S_R$ . Combining this representation with  $\Psi_r$  yields

$$V(x_i, f) = \frac{i\kappa \mathcal{V}_T(f) \mathcal{V}_R(f)}{4\pi^2} \int_0^{2\pi} d\phi \int_0^{\pi/2 - i\infty} R(\theta, f) F_T(\theta, \phi) F_R(\theta, \phi) \sin \theta d\theta, \quad (1)$$

where  $F_{T,R}(\theta, \phi)$  are the transmitter and receiver directivity functions.  $\mathcal{V}_{T,R}(f)$  is the frequency-dependent particle velocity on the transmitter or receiver surface when either operates as a transmitter, and  $R(\theta, f)$  is the reflection coefficient. Then,  $\theta$  and  $\phi$  are polar and azimuthal angles,  $f$  is the frequency,  $\kappa$  is the wavenumber in the fluid.

Our problem now reduces to one of obtaining sufficiently accurate estimates of the transducer directivity functions  $F_T(\theta, \phi)$  and  $F_R(\theta, \phi)$ . There are several ways to proceed. Since we employ mechanically damped PZT-5 transducers for essentially all measurements, perhaps the most accurate approximation would be the familiar field expression for a baffled circular piston radiator. By reciprocity,  $F_T(\theta, \phi)$  and  $F_R(\theta, \phi)$  are equal, and we may write the receiver voltage  $V(x_i, f)$  as a function of transducer position and spatial and frequency response as

$$V(x_i, f) = 2i\kappa\mathcal{V}_T(f)\mathcal{V}_R(f)a^4 \int_0^{\pi/2-i\infty} R(\theta, f)e^{i\kappa\rho\cos(\theta-\theta_0)} \sin\theta d\theta \\ \times \int_0^\pi \left[ \frac{J_1(\kappa a \sin\delta)}{\kappa a \sin\delta} \right]^2 \exp[-i\kappa\rho \sin\theta_0 \sin\theta(1-\cos\phi)] d\phi. \quad (2)$$

Here,  $\rho$  is the separation of the transducer centers measured through the origin of coordinates, as shown in Fig.1,  $J_1(\kappa a \sin\delta)$  is the first order Bessel function,  $\delta$  is the angle between the wavevector of the spectral component at  $(\theta, \phi)$  and the transducer acoustical axis.

While the Bessel function expression of Eq. (2) is a reasonably accurate representation of the directivity function for a damped commercial ultrasonic probe, it is only one possible choice to approximate the experimental beam. Another often used approximation is the Gaussian beam [6,7,8], favored not so much for its fidelity as for its advantageous transformation properties. We have found that the theoretical prediction of transducer voltage is almost completely insensitive to the substitution of Gaussian beams in Eq. (1) for the piston beam, so long as the experiment consists of identical transmitter and receiver transducers and  $\kappa a > 1$ . This substitution works because the piston transducers are used for generation *and* detection, and in that case the spatially convolved Gaussian beams become an excellent approximation for the combined pistons, even in the nearfield.

Substituting the Gaussian directivity functions for  $F_T$  and  $F_R$  in Eq. (1), the integral can be conveniently performed asymptotically by a steepest descent evaluation along a deformed contour in the complex  $\theta$  plane. When the saddle point closely approaches or coincides with a pole of the reflection coefficient, additional actions must be taken to accommodate this situation [11]. Aspects of this problem can be interpreted as a geometric argument. In Fig.1 the distance from the transmitter center to the origin (labeled  $\rho/2$ ) and returning to the receiver center is the specular ray associated with the saddle point of the  $\theta$  integration in Eq. (1). Likewise, the ray incident at a leaky wave angle in Fig.1 corresponds to a pole of the RC and can be independently associated with that contribution to Eq. (1). An exception occurs when the saddle point and pole exactly, or nearly, coincide.

In most practical cases it is sufficient to investigate the solution of the saddle point equation for  $x_i \ll \rho$ . In that case the asymptotic saddle point solution is

$$\theta_s \approx \alpha + \frac{x_i \cos\alpha}{\rho(1+4\gamma^2)}(1+2i\gamma). \quad (3)$$

This expression includes all geometrical parameters of the system. Thus, the effect of changing the transducer parameters  $x_i$ ,  $\alpha$ ,  $\rho$ ,  $a$ ,  $f$ , or ( $\gamma \sim \kappa a^2/\rho$ ) is mathematically equivalent to shifting the saddle point  $\theta_s$  in the complex  $\theta$  plane.

In the leakage region ( $x_i > 0$ ) the imaginary part of  $\theta_s$  moves toward the positive imaginary direction from the real axis in the complex  $\theta$  plane and moves closer to the

RC poles, denoted  $\theta_p$ . As  $\theta_s$  approaches a pole, the effect of a plate mode on the reflected field increases. For  $x_i < 0$  the distance between  $\theta_s$  and the poles increases, and the specular component dominates the receiver voltage. The saddle point is entirely real only when  $x_i = 0$ , or when the amplitude maximum and stationary phase point coincide, *ie.* when  $\theta_0 = \alpha$ . However, this condition does not imply optimum mode coupling, which occurs instead when  $|\theta_p - \theta_s|$  is minimum.

With the calculation of the saddle point position it is possible to evaluate the reflection integral as sum of saddle point and RC pole contributions in the form of a uniform asymptotic solution, such as suggested by [11]. Following [6,7,8] and others, the RC contributions to the reflected field come essentially only from the singularities or poles. Therefore,  $R(\theta, f)$  can be written

$$V(x_i, f) = \frac{\pi \alpha^4 \mathcal{V}_T(f) \mathcal{V}_R(f)}{2\rho(i + 2\gamma)} \exp[i\Phi - (x_i/x_\ell)^2] \times \left\{ 1 - \sqrt{\pi \kappa \rho(i/2 + \gamma)} \sum_{j=1}^n \theta''_{pj} \omega(\sqrt{\kappa \rho(i/2 + \gamma)}(\theta_{pj} - \theta_s)) \right\}, \quad (4)$$

where  $\Phi$  is a phase function, and  $x_\ell$  is a beam localization parameter given by  $x_\ell = ab\sqrt{1 + 4\gamma^2}/(\gamma \cos \alpha)$ . The structure of the expression in Eq. (4), with specular and leaky wave terms, is similar to those of both Bertoni and Tamir [6] for the halfspace and Pitts, *et al.* for the plate [7]. The essential difference is that Eq. (4) models the observed voltage for identical transmitter and receiver.

## RESULTS AND DISCUSSION

According to Auld's reciprocity principle [10] it is possible to consider the output signal dependence as an interaction between two acoustical fields on the plate surface: one from the reflected field created by transmitter, and the other the incident field created by the receiver when it functions as a transmitter. In the figures below, the received voltage  $V(x_i, f)$  is presented at a fixed incident angle  $\alpha$  as a coherent sum of specular (dashed) and leaky wave (dotted) components and labeled 1 and 2, respectively. The sum is denoted by the solid curves and labeled 3. The vertical dashed lines labeled with a plate mode indicate the position of RC zeroes. We denote a positive beam shift  $x_i$  when the transducers' acoustical axes intersect at a point located below the upper plate surface, and negative otherwise.

In Fig.2a we plot the  $V(x_i, f)$  dependence calculated from Eq. (4) for a negative beam shift of  $x_i = -10$  mm, where the sample is a 1.51 mm thick steel plate. The transducer axes are in the  $xz$  plane and oriented to incident angles of  $\alpha=25^\circ$ . For this transducer position only the influence of the  $S_0$  mode on the received voltage is pronounced. The reason for this behavior is illustrated in Fig.2bc, where the beams are represented schematically. With a negative beam shift, the effect of two additional modes,  $A_1$  and  $S_1$ , on the signal is very weak because they occur at higher frequencies, where the diffraction-limited beam footprint leaves almost no overlap, as in Fig.2c. For low frequencies, the sizes of the two footprints on the plate are larger because the beams spread as they propagate from the transducers. A similar geometrical argument can be made to explain the frequency dependence of the voltage signal for positive  $x_i$ .

Calculated results for the same plate with  $x_i=+12$  mm are presented in Fig.3a. For the  $S_0$  mode the coherent sum at low frequency yields a minimum in  $V(x_i, f)$  very

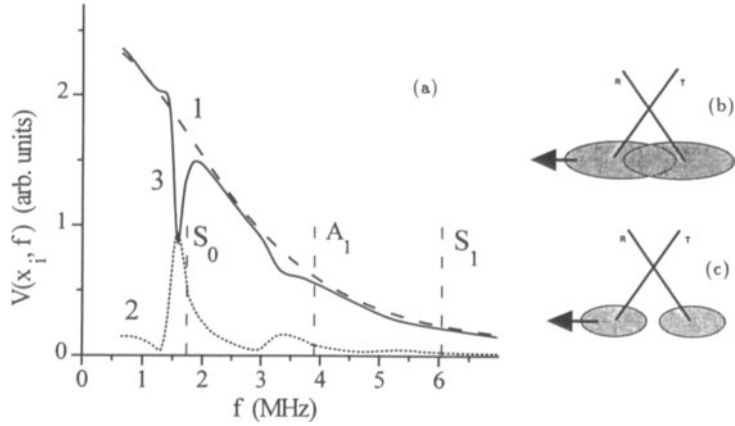


Figure 2: (a) Receiver voltage vs frequency for beam shift  $x_i = -10$  mm. Dashed curve (1) is specular component, dotted curve (2) is leaky wave, and solid curve (3) is total voltage. Reflection coefficient zeroes denoted by vertical dashed lines and labeled with mode designation. Schematic illustration of diffraction effects and beam overlap at low (b) and high (c) frequency for negative beam shift,  $x_i < 0$ .

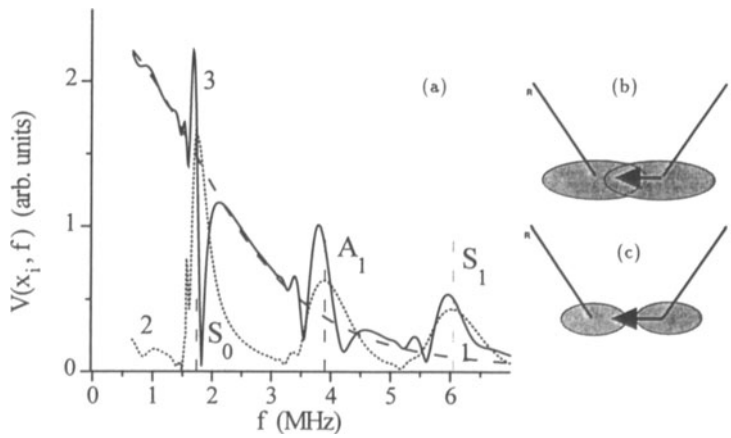


Figure 3: (a) Receiver voltage vs frequency for beam shift  $x_i = +12$  mm, showing the effect of diffraction on voltage minima. Dashed curve (1) is specular component, dotted curve (2) is leaky wave, and solid curve (3) is total voltage. Reflection coefficient zeroes denoted by vertical dashed lines and labeled with mode designation. Schematic illustration of diffraction effects and beam overlap at low (b) and high (c) frequency for positive beam shift,  $x_i > 0$ .

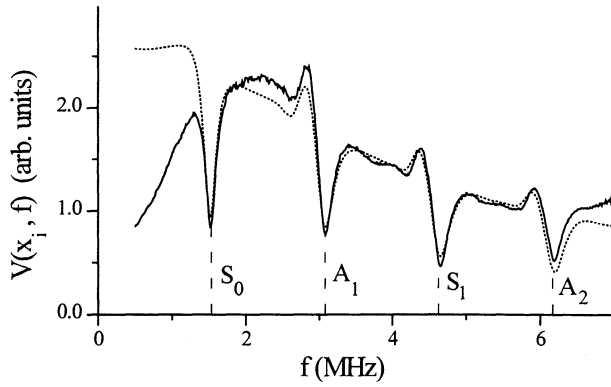


Figure 4: Experimental (solid curve) and theoretical (dotted curve) receiver voltage for a two-transducer frequency scan at  $\alpha = 20^\circ$  and  $x_i = +5$  mm. Reflection coefficient zeroes denoted by vertical dashed lines and labeled with mode designation.

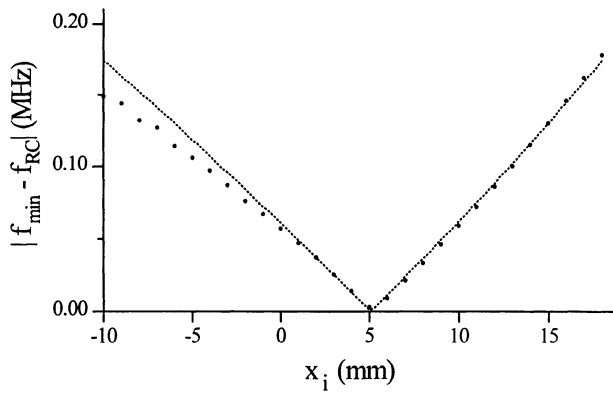


Figure 5: Absolute value of frequency difference  $f_{min} - f_{RC}$  between voltage minimum and corresponding RC zero for the  $S_0$  guided wave mode at an incident angle of  $\alpha = 25^\circ$ . Discrete points are the exact expression, and the curves are the approximate values;  $f_{min} < f_{RC}$  for values of  $x_i$  to the left of minimum.

near the corresponding RC zero. At higher frequencies, however, these effects produce a *maximum* in  $V(x_i, f)$ , instead of a minimum, at the  $A_1$  and  $S_1$  modes for beam shifts larger than the transducer diameter  $2a$ . The beam geometry, illustrated in Fig.3 b and c, shows this dependence on beams footprints schematically.

These observations have substantial significance for the design of experiments intended to deduce plate properties from measurements of the voltage on the receiving transducer in reflection. From Fig.2 and Fig.3, it is clear that the association of reflection minima with zeroes of the reflection coefficient must be performed with care. In neither case, for  $x_i = -10$  mm or  $+12$  mm, are the  $A_1$  or  $S_1$  zeroes accompanied by clearly defined reflection minima, as measured in the receiver voltage. There exists, however, a range of beam shift  $x_i$  and frequency  $f$  where such measurements can be reliably made.

In Fig.4,  $x_i = +5$  mm, and the solid curve is the experiment, and the dotted curve is the calculated voltage from Eq. (4). Deep, well defined minima accompany each Lamb mode, from  $S_0$  to  $A_2$ , excited by the incident beam. Moreover, the minima align very well with the RC zeroes (denoted by vertical dashed lines), and the entire curve, including all details of the behavior, is well modeled by the theory. Interestingly, a small positive beam shift, about the size of the transducer radius, yields the closest correlation between observed voltage minima and RC zeroes. These comments are especially applicable for a frequency range in which the parameter  $2a/\lambda$  varies from about 5 to about 40, with the water path close to the Rayleigh distance.

Figs. 2 through 4 demonstrate that the frequency  $f_{min}$  which produces a reflection minimum in the voltage  $V(x_i, f)$  will not generally coincide with its RC zero  $f_{RC}$ . As discussed above, the relative phases of the specular and leaky wave signal components are dependent on the beam shift  $x_i$ . In addition, we note that the saddle point  $\theta_s$  is also dependent on this parameter. For a given mode at a given incident angle  $\alpha$  and frequency  $f$  therefore, there exists an optimum value of  $x_i$  which yields not only the minimum voltage  $V(x_i, f)$ , but which also coincides with the RC zero.

The frequency difference  $f_{min} - f_{RC}$  between the observed voltage minimum and the corresponding RC zero as a function of  $x_i$  is presented in Fig.5, shown as a dotted curve, for the  $S_0$  mode at an incident angle of  $25^\circ$ . The discrete points in these plots denote the same quantity calculated from minima found using the full voltage expression in Eq. (4) for several values of  $x_i$ .

## SUMMARY

This article presents an accurate, approximate analysis for the receiver voltage in a geometry with bounded acoustic beams reflected from fluid-loaded structures. The relationship between reflection coefficient poles and transducer voltage minima is calculated and discussed. A series of precision experiments on a uniform, homogeneous plate is shown to validate the calculation. These results have significance for material property extraction from reflection measurements on fluid-loaded structures.

## ACKNOWLEDGEMENTS

This work performed with partial support from Naval Surface Warfare Center (Carderock Div.).

## REFERENCES

1. D. C. Worlton, Experimental confirmation of Lamb waves at megacycle frequencies, *J. Appl. Phys.* 32, 967-971 (1961).
2. M. Hattunen and M. Luukkala, An investigation of generalized Lamb waves using ultrasonic measurements, *Appl. Phys.* 2, 257-263 (1973).
3. A. H. Nayfeh and D. E. Chimenti, Ultrasonic wave reflection from liquid-coupled orthotropic plates with application to fibrous composites, *J. Appl. Mech.* 55, 863-870 (1988).
4. M. Deschamps and B. Hosten, The effects of viscoelasticity on the reflection and transmission of ultrasonic waves by an orthotropic plate, *J. Acoust. Soc. Am.* 91, 2007-15 (1992).
5. A. Schoch, Sound transmission through plates, *Acoustica* 2, 1-18 (1952).
6. H. L. Bertoni and T. Tamir, Unified theory of Rayleigh-angle phenomena for acoustic beams at liquid-solid interfaces, *Appl. Phys.* 2, 157-172 (1973).
7. L. E. Pitts, T. J. Plona, and W. G. Mayer, Theory of nonspecular reflection effects for an ultrasonic beam incident on a solid plate in a liquid, *IEEE Trans. Sonics Ultrason.* SU-24, 101-109 (1977).
8. L. B. Felsen, and S. Zeroug, Nonspecular reflection of beams from liquid-solid interfaces, *J. Nondestruct. Eval.* 11, 263-278 (1992).
9. D. E. Chimenti, A. Safaeinili, and O. I. Lobkis, Quantitative materials characterization of elastic plates using air-coupled leaky Lamb waves, these proceedings.
10. B. A. Auld, General electromechanical reciprocity relations applied to the calculation of elastic wave scattering coefficients, *Wave Motion* 1, 3-10 (1979).
11. L. B. Felsen and N. Marcuvitz, *Radiation and Scattering of Waves*, Prentice-Hall, Englewood Cliffs, NJ (1973).